

# Study of ac conductivity and dielectric properties of composites of Poly (Vinyl Alcohol) (PVA) and Reduced Graphene Oxide (RGO)

Dr. Geeta Kandhol

\*Corresponding Author: Email: geeta.kandhol.123@ gmail.com (Geeta Kandhol)

---

## **Abstract**

The composite films of Poly (vinyl alcohol) (PVA) and Reduced graphene oxide (RGO) with a with 1 wt% and 2 wt% loading of RGO using solution mixing have been prepared via evaporative casting technique. The variation in ac conductivity and dielectric loss parameter ( $\epsilon''$ ) with frequency (100 kHz- 1.5 MHz) has been studied at different temperatures (320K to 400K) in order to estimate the activation energy and barrier height. The almost linear variation in ac conductivity ( $\sigma_{ac}$ ) with frequency at each studied temperature suggests the observation of universal power law in these composites. The slope of these curves was found to decrease with rise in temperature depicting the Correlated Barrier Hopping (CBH) model as charge transport mechanism in these composites. Moreover the variation in ac conductivity with frequency for the composites also suggests that conduction is via hopping of charge carriers. The values of  $\epsilon'$  and  $\epsilon''$  have been found to increase with rise in temperature and loading of RGO and maximum barrier height is found to be decreased with increasing concentration of RGO.

**Keywords:** PVA, RGO, composite, dielectric properties, activation energy, barrier height

---

Date of Submission: 24-01-2023

Date of acceptance: 07-02-2023

---

## **I. Introduction.**

Polymers with good dielectric properties are preferred to conventional dielectric materials which are usually ceramic based with serious environmental issue.<sup>i</sup> In this respect, study of dielectric behavior of poly (Vinyl Alcohol) PVA based composites have attracted attention due to various technological applications of these composites in the electronic and optoelectronic fields<sup>ii,iii,iv</sup> [ ]. After the discovery of graphene which is a single layer of carbon atom arranged in honeycomb lattice<sup>v</sup> [ ], a continuous research is going in graphene related material. This is attributed due to its various extraordinary properties like high charge carrier mobility at room temperature<sup>vi</sup> [ ], large theoretical area and high electronic conductivity<sup>vii</sup> [ ] which are also reflected in graphene grafted polymer composites. Due to these unique properties, PVA-graphene composites are expected to have improved dielectric properties viz ac conductivity, dielectric constant and dielectric loss. In polymeric material, the measurement of dielectric permittivity and ac conductivity generally shows dispersion behavior with frequency and temperature.<sup>viii,ix,x</sup> Thus study of the dielectric properties is crucial for the analysis of various physical properties of the composite material. Also it provides a fundamental way to understand the nature of conduction and defects in any composite material. Here we report the temperature and frequency dependence of dielectric constant ( $\epsilon'$ ), dielectric loss ( $\epsilon''$ ) and ac conductivity ( $\sigma_{ac}$ ) for PVA-Reduced graphene oxide (RGO) composite films prepared via solution mixing and evaporative casting technique. As a consequence of addition of RGO in PVA, a number of interface regions and thermal activated charge carriers may get increased which leads to the changes in dielectric as well as electrical properties. Further ac conductivity of most of the complex polymeric material is found to obey Joncher universal dielectric response (UDR) law given by the formula<sup>xi</sup>  $\sigma_{ac}(\omega) = A\omega^s$  where A is constant and s is the exponent parameter which depends upon temperature and frequency and is a measure of degree of interaction between various constituents of composite material. Thus conduction mechanism is studied by analyzing the variations in s parameters with frequency and temperature. Here main objective of the work is to study the effect of RGO loading on dielectric function and ac conductivity in composite system. Further activation energy and barrier height of these composites are inferred from these parameters.

## II. Experimental Section

### 2.1 Materials and methods

Poly (vinyl alcohol) (PVA) powder, graphite powder, concentrated Sulphuric Acid (H<sub>2</sub>SO<sub>4</sub>), Potassium Permanganate (KMnO<sub>4</sub>), Sodium Nitrate (NaNO<sub>3</sub>), Hydrogen Peroxide (H<sub>2</sub>O<sub>2</sub>), Hydrochloric Acid (HCl), Hydrazine Hydrate (N<sub>2</sub>H<sub>4</sub>) and Ammonia solution were used as they are procured.

#### 2.1.2 Synthesis of RGO

In order to synthesize the Poly (Vinyl alcohol) (PVA) - reduced graphene oxide (RGO) composite films, firstly RGO was prepared by chemical reduction of graphite oxide (GO) using modified Hummer's<sup>xii</sup> method. For the preparation of RGO, an equal amount of GO powder was dispersed in DI, followed by mixing of 10 µl of hydrazine hydrate in it. Ammonia solution was added to keep the pH level of mixture at 10. After that solution is heated at 100°C in oil bath for next 2 hours under stirring resulting in formation of reduced graphene oxide (RGO) dispersion.

#### 2.1.2 Preparation of PVA-RGO composites

In order to synthesized the composite films of as-prepared RGO with PVA, the PVA solution was prepared by dissolving 2 gm of PVA powder in 40 ml of DI under stirring. After this, 50 ml of RGO solution was added to 10 ml of PVA solution under sonication followed by stirring giving the homogeneous composite solution of PVA-RGO with 1 wt. % of RGO. Then solution mixture was casted on teflon petri-dish and allowed for evaporation of residual solution at room temperature to obtain free standing films. In the similar manner composite films of 2 wt. % of RGO in PVA were prepared by adding the desired volume of as prepared RGO solution in PVA solution. The thickness of the obtained free standing films was measured using digital screw micrometer of least count 0.001 mm and found to be around 20±5 micron in average.

### 2.2 Characterizations

The nature of optical transitions in as-prepared graphene oxide (GO), reduced graphene oxide (RGO) and PVA-RGO composite films were studied using Shimadzu Double Beam Double Monochromator UV-Visible Spectrophotometer (UV-Visible 2550) operating in wavelength range from 190-900 nm with a resolution of ±0.1 nm. Transmission Electron Microscopy (TEM) (Tecnai G2 20 TEM) operating at 200kV was utilized for morphological study of as-prepared RGO. The temperature dependent dielectric measurements of PVA and PVA-RGO composite films were performed as a function of frequency (100 kHz-1.5MHz) in the temperature range of 320-400K using Agilent-E4980A LCR meter having a Lakeshore 325 temperature controller and interfaced via a Lab-View program. From the measured value of Capacitance (C) and dielectric loss (tanδ) of the samples, the real part (ε') and imaginary part (ε'') of dielectric constant has been determined through the formulae,  $\epsilon' = (C*d)/(\epsilon*A)$  and  $\epsilon'' = \epsilon' * \tan\delta$ ; where d is thickness of sample and A is the area of electrode on the sample. The value of ac conductivity ( $\sigma_{ac}$ ) is determined from the formula,

$$\sigma_{ac} = 2\pi f \epsilon_0 \epsilon''$$

## III. Results and discussion

### 3.1 GO and RGO

The UV-Visible absorption spectrum of as-prepared GO and RGO dispersion in DI is shown in Figure 1. In this figure, the absorption peak around 232 nm (curve 'a') corresponds to the  $\pi$ - $\pi^*$  transition in C-C and C=C bonds present in functional group of GO. Also, hump at around 300 nm is attributed to the n- $\pi^*$  transition of C=O bond in GO<sup>xiii</sup> [ ]. The peak corresponding to  $\pi$ - $\pi^*$  transition in GO shifted to 273 nm in RGO (curve 'b'). This can be ascribed due to the interband excitonic transition<sup>xiv</sup> [ ], thus depicting the formation of graphene like structure<sup>xv</sup> [ ] after oxidation-reduction process of GO.

Figure 2 represents the TEM image of as-prepared RGO. It is clear from this image that the morphology of the prepared RGO is ribbon like with many folds and wrinkles<sup>xvi</sup>[ ]. These wrinkles are manifestation of defects produced due to oxidation-reduction process during synthesis.

Raman spectra of Graphite, GO and RGO is shown in figure 3. In graphite, an intense peak at 1577 cm<sup>-1</sup> corresponds to G band. This peak is observed in all poly-aromatic hydrocarbon materials as reported in literature.[ ] Also another small peak appearing nearly at 1361 cm<sup>-1</sup> may be attributed to D band of graphite. Ratio of intensity of D (I<sub>D</sub>) and G (I<sub>G</sub>) peak is found to be equal to 0.092 which suggest that graphite used is almost defect free. These two corresponding peaks in case of GO appear at 1587 cm<sup>-1</sup> and 1344 cm<sup>-1</sup> respectively. Clearly, position of G peak in GO there is a blue shift of 10 cm<sup>-1</sup> corresponding to G peak in GO as compared to graphite which indicates the decreased size of crystallite during oxidation.[ ]Further the ratio I<sub>D</sub>/I<sub>G</sub> is inversely proportional to size of sp<sup>2</sup> crystallite domain. The intensity ratio I<sub>D</sub>/I<sub>G</sub> is found to smaller in case of RGO ( ) as compared to GO ( ) indicating the decreased size of sp<sup>2</sup> domains during reduction as an effect of heat treatment. This is consistent with the previous reports.[ ]

### 3.2 PVA-RGO composite films

#### 3.2.1 UV-Visible absorption spectroscopy

Figure 3 represents the UV-Visible absorption spectra for pure PVA and PVA-RGO composite films with 1 and 2 wt% loading of RGO. It is clearly observable from curve 'a' of this figure that PVA exhibits almost no absorption in the entire UV range except the appearance of absorption band edge peaking around 213 nm and small absorption band at 276 nm, which may be assigned to  $n-\pi^*$  transitions related to the carbonyl group (C=O) present in PVA<sup>xvii</sup> [ ]. However, in composite samples, the characteristic absorption of RGO around 271 nm starts appearing and overshadows the absorption observed due to pure PVA (curve 'b to d'). Further, the intensity of this absorption peak increases along with small blue shifting with increase in loading of RGO. The blue shifting in peak clearly indicates formation of some bonding between RGO layers and PVA chains.

#### 3.2.2 Frequency and temperature dependence of ac conductivity

The variation of  $\ln(\sigma_{ac})$  with  $\ln(f)$  is shown in figure 4 for PVA and PVA-RGO composites at different elevated temperatures. It is clear from figure that dispersion of  $\ln(\sigma_{ac})$  with  $\ln(f)$  is almost linear with two different slopes in lower and higher frequency region for both pure PVA and composite films. However at higher temperature, value of slopes becomes almost same for both low and high frequency region. Values of frequency exponent  $s$  parameter have been calculated from slope of  $\sigma_{ac}$  curves (figure 4) and plotted as a function of temperature in both low and high frequency regions (figure 5). It is clear from figure that values of  $s$  parameter lies between 0 and 1 and decrease with increase in temperature for both low and high frequency. For example, the value of  $s$  parameter decreases from 0.75 to 0.16 for pure PVA and from 0.77 to 0.26 for PVA with 2 wt% of RGO loading in PVA in low frequency region. This behavior is analogous to that observed in amorphous semiconductor and glasses<sup>xviii, xix</sup> [ ] and may be attributed to correlated barrier hopping (CBH) conduction mechanism.

Further with the addition of RGO in PVA, value of ac conductivity increases at low frequency due to increased  $\sigma_{dc}$ <sup>xx</sup> [ ] which can be attributed to formation of conductive networks due to presence of RGO.

The variation of ac conductivity with temperature at different frequencies for PVA and PVA-RGO composites is shown in figure 6 where  $\ln(\sigma_{ac})$  is plotted as a function of  $1000/T(K^{-1})$ . It is clear from figure 6 that  $\sigma_{ac}$  has dependence of both temperature and frequency in entire range and the relation is linear with two different slopes depicting two different activation energy regions. This kind of behavior is further similar to amorphous semiconductor and glasses<sup>xxi</sup> [ ]. Accordingly frequency dependent ac conductivity can be expressed as sum of two different conduction mechanisms, one with weak temperature dependence which can be considered due to hopping of charge carriers over barrier between different sites and other with strong temperature dependence. The value of activation energy at various frequencies can be determined from slopes of  $\ln(\sigma_{ac})$  versus  $1000/T$  curve using well known expression  $\sigma_{ac}(\omega) = \sigma_0 \exp(\Delta E_a(\omega) / k_B T)$  where  $\sigma_0$  is a constant,  $\Delta E_a(\omega)$  is activation energy for conduction,  $k_B$  is Boltzmann constant and  $T$  is absolute temperature. The frequency dependence of activation energy for PVA and PVA-RGO composites is shown in figure 7. It is evident that activation energy decreases with increasing frequency for all samples. This behavior is similar to that of shown by various other material<sup>xxii, xxiii</sup>. The small values of activation energy and increase in ac conductivity with increasing frequency for all samples assures that dominant conduction mechanism is hopping of charge carriers.

#### 3.2.3 Frequency and temperature dependence of dielectric constant and dielectric loss

It is clear from frequency dispersion of the real ( $\epsilon'$ ) and imaginary ( $\epsilon''$ ) parts of the dielectric permittivity (figure 8 and 9) that both  $\epsilon'$  and  $\epsilon''$  decrease with increase in frequency for PVA and PVA-RGO composites thereby depicting the characteristic dielectric behavior of polymers called Maxwell-Wagner-Sillars polarization<sup>xxiv</sup> [ ]. This decrease in values is due to inadequacy of dipoles to follow the orientations of applied electric field with increasing frequencies. Therefore, their contribution toward net dipole moment decreases which results in lowering the value of  $\epsilon'$  and  $\epsilon''$ . Further with rise in temperature, the value of  $\epsilon'$  has been observed to increase at all frequencies in all samples. This can be attributed to the increase in thermal kinematics of charge carriers which may facilitate the faster dipole orientation, there by decrease in polarization resistance at higher temperature<sup>xxv</sup> [ ]. Also, it is found that the value of  $\epsilon'$  rises in composite films with increase in RGO concentration at all frequencies and at all studied temperature which can be explained by the theoretical model proposed by Vo and Si<sup>xxvi</sup> [ ]. This model may be used to estimate the complex dielectric permittivity ( $\epsilon^*$ ) of dielectric material as an effect of formation of interface region due to conductive filler reinforcement in insulating matrix. Further the increased loading of RGO inside the composite matrix may result in increased free charge carriers and thus value of  $\epsilon^*$  begins to rise.

However increase in value of  $\epsilon''$  with rise in temperature is more significant at low frequency region. At low frequencies, the rise in dielectric loss with increase in temperature may be due to increased conductivity

of PVA-RGO<sup>xxvii</sup> []. At higher frequency, the small value of dielectric loss is observed which remains almost steady in this range. The observed small values of  $\epsilon''$  in these composite samples signify that these can be used as non-lossy dielectric material in higher frequency range.

Further based upon theoretical model of hopping of charge carriers over a potential barrier<sup>xxviii</sup> [], dielectric loss can be expressed as  $\epsilon''=A\omega^m$  where A is constant and m is the frequency power parameter and is given by  $m = -4k_B T/W_m$  where  $W_m$  is the maximum barrier height and T is the absolute temperature. Values of m at different temperatures can be found from the slope of  $\ln(\epsilon'')$  versus  $\ln(\omega)$  curve. Figure 10 shows the variation of m with temperature for PVA and PVA-RGO composites. It is clear from the figure that value of m decreases linearly with temperature for all samples. The value of maximum barrier height for samples is shown in table 1. Clearly the value of  $W_m$  decreases with increase in concentration of RGO in PVA.

#### IV. CONCLUSIONS

PVA and PVA-RGO composite films were synthesized by solution cast method. Ac conductivity and dielectric properties of these prepared samples were studied in the frequency range of 100 kHz-1.5MHz and temperature range 320-400K. Both dielectric constant and dielectric loss increase with increasing temperature and decreases with increase in frequency through the studied range of temperature and frequency. Value of frequency exponent parameter (s) with increasing temperature is found to be decreased for all samples which indicates correlated barrier hopping model. Further small value of ac conductivity also suggests the hopping of charge carriers as conduction mechanism. Also with increasing concentration of RGO, value of maximum barrier height decreases.

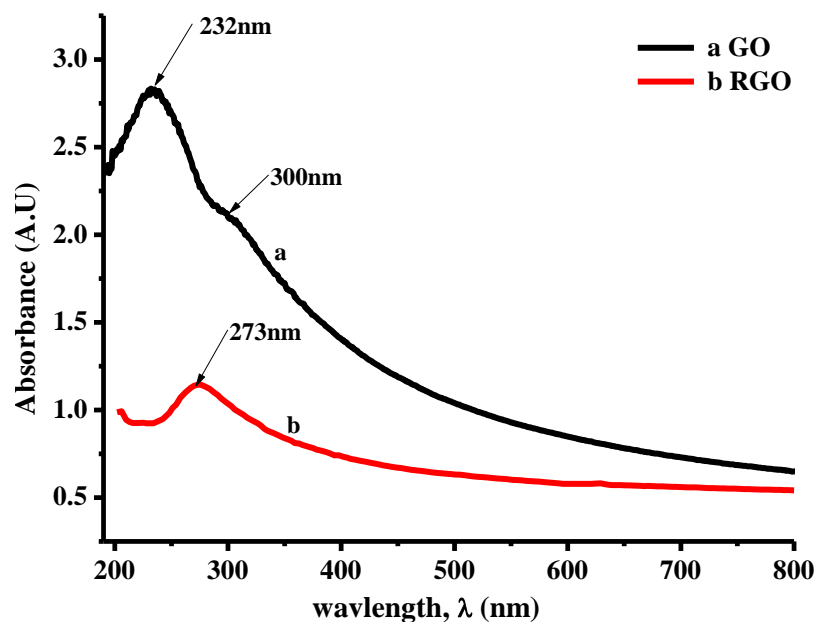


**Figure 1** UV-Visible spectra of GO and RGO

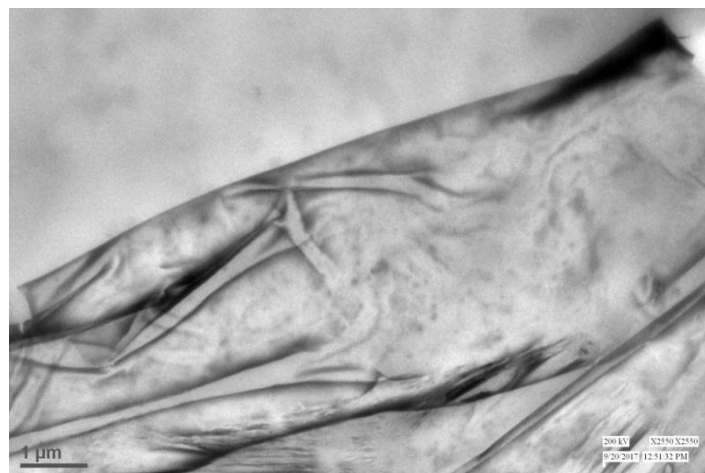


**Figure 2** TEM image of RGO

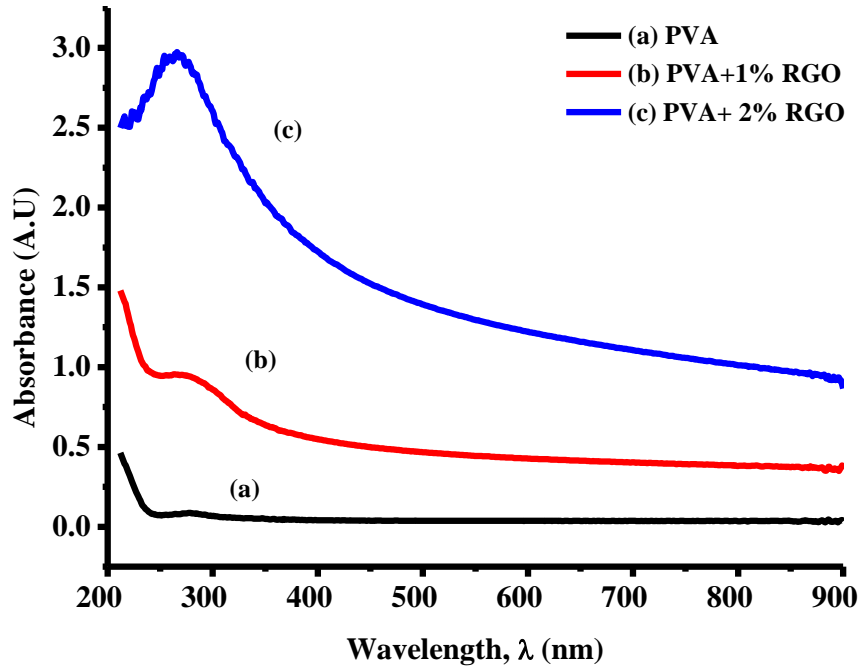
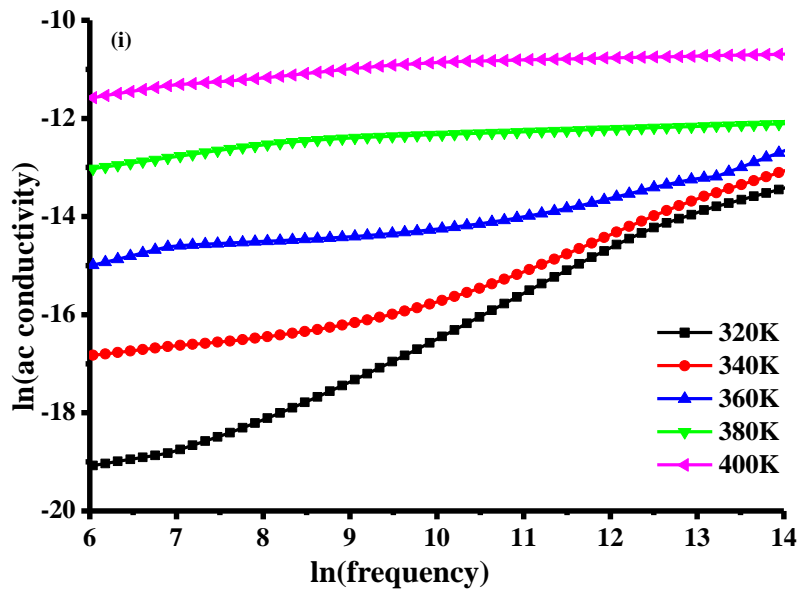


Figure 3 UV-Visible spectra of PVA and PVA-RGO composites



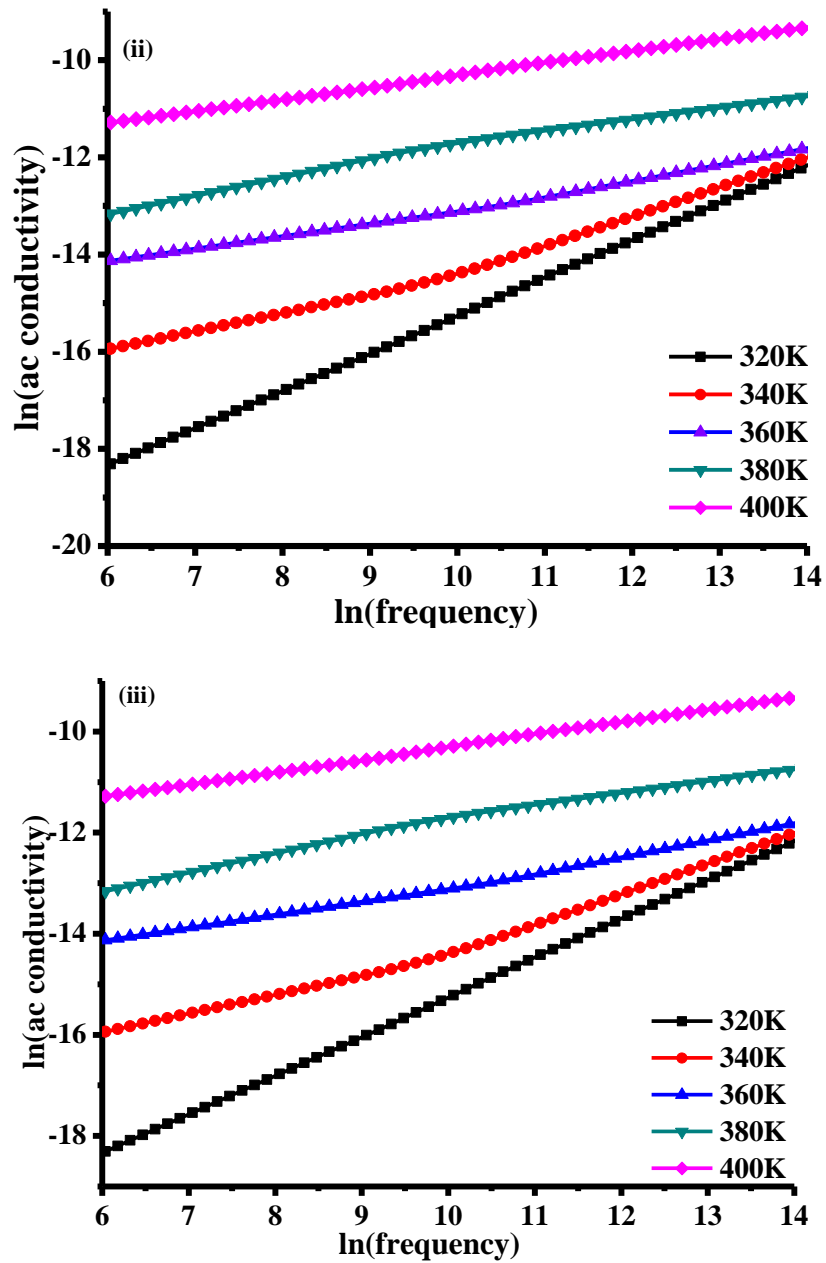


Figure 4 Frequency dependence of  $\sigma_{ac}$  at different temperatures

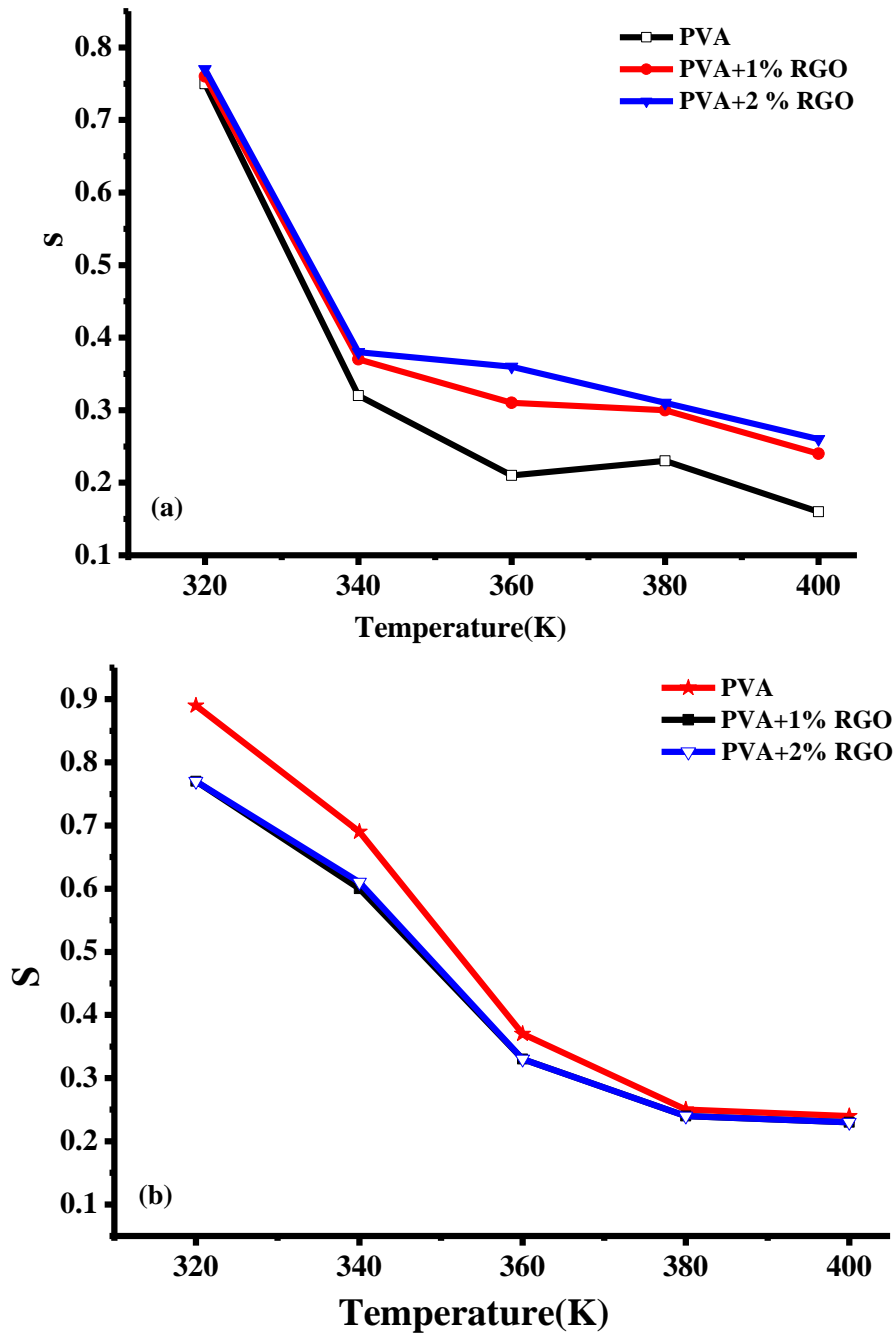
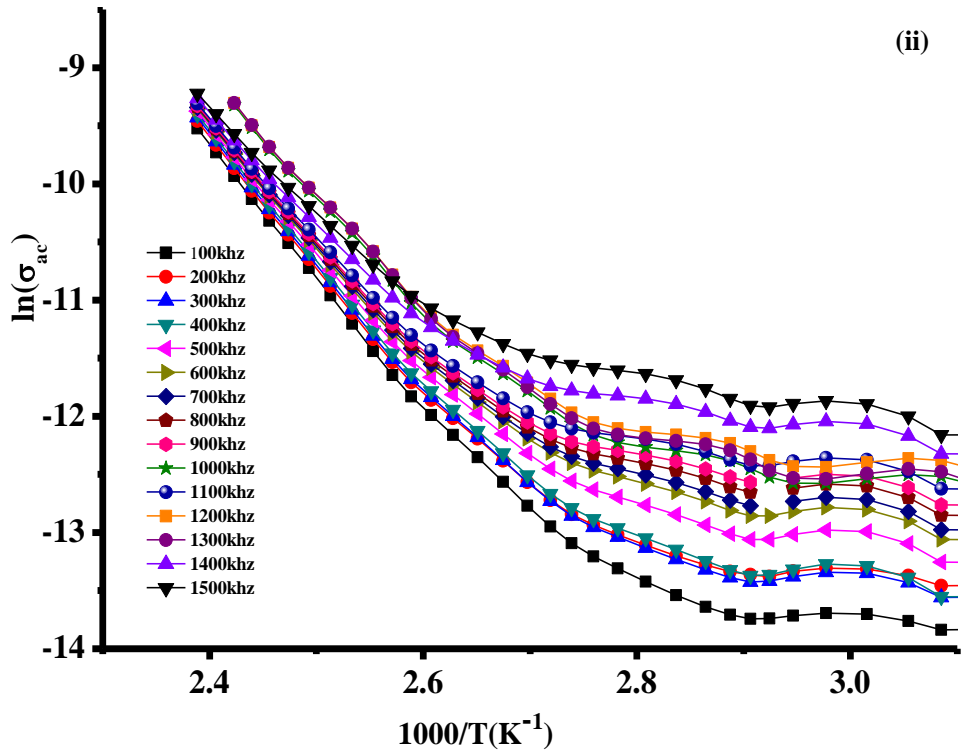
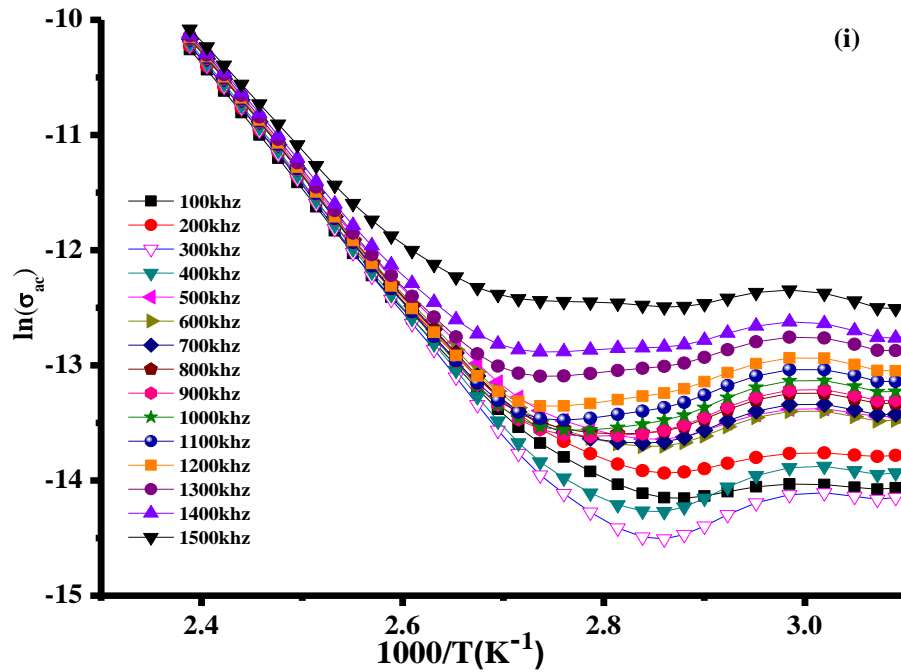


Figure 5 Temperature dependence of frequency exponent parameter ( $s$ ) for PVA and PVA-RGO composites in (a) low frequency region (b) high frequency region



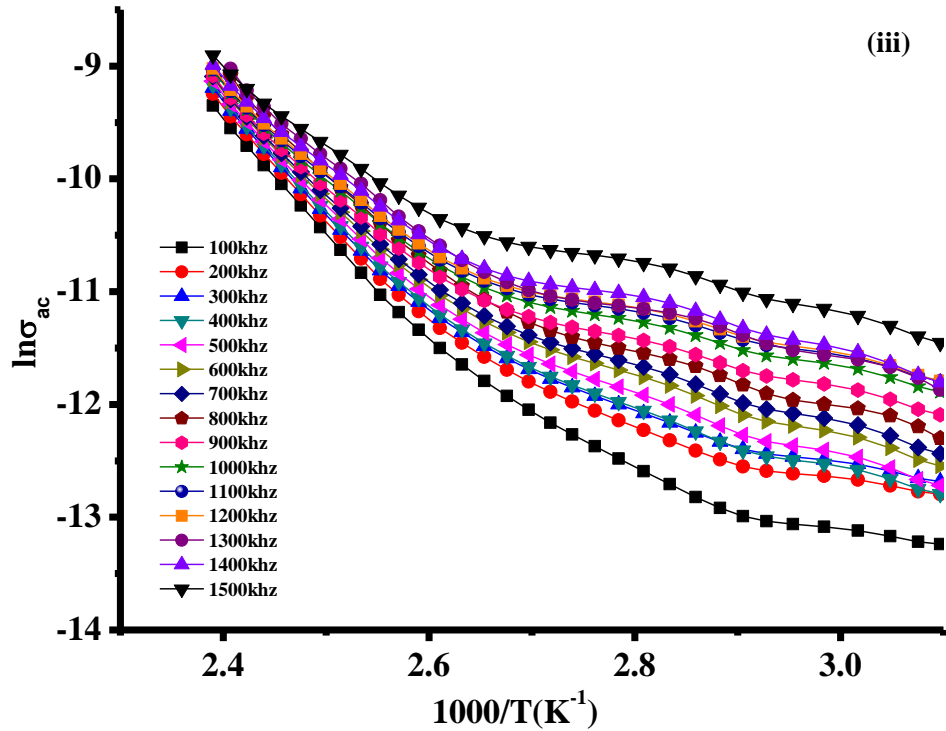


Figure 6 Temperature dependence of  $\sigma_{ac}$  for (i) PVA (ii) PVA+1%RGO (iii) PVA+2%RGO at different frequencies

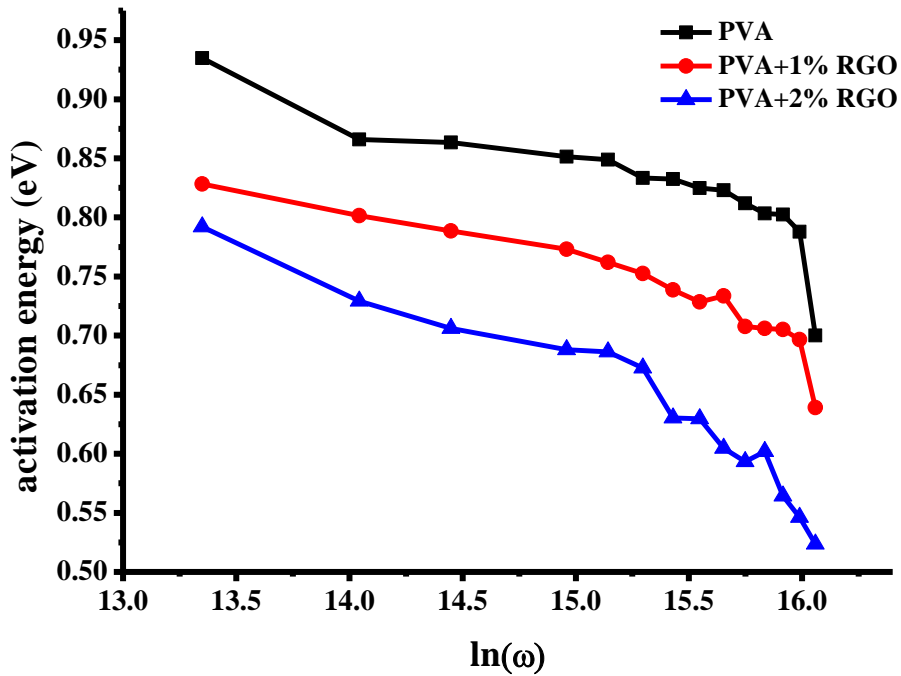
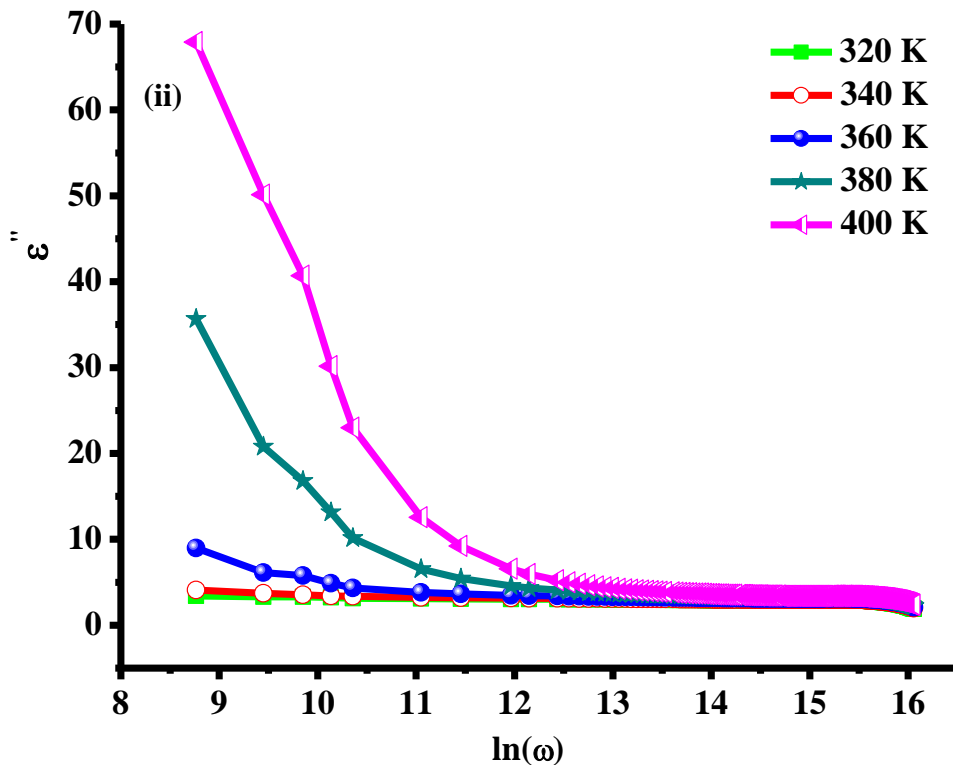
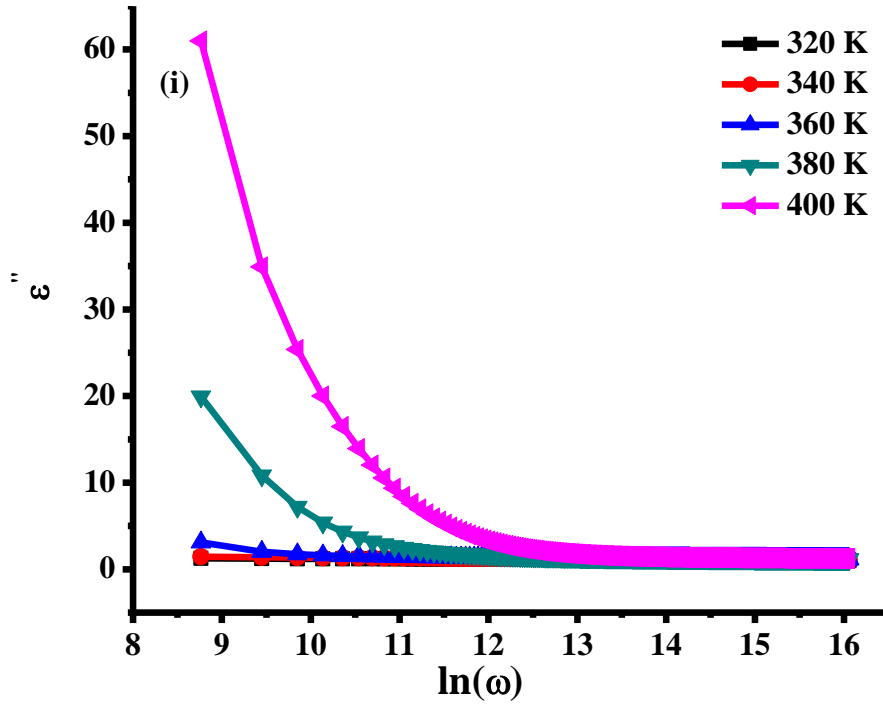


Figure 7 Frequency dependence of activation energy for PVA and PVA-RGO Composites



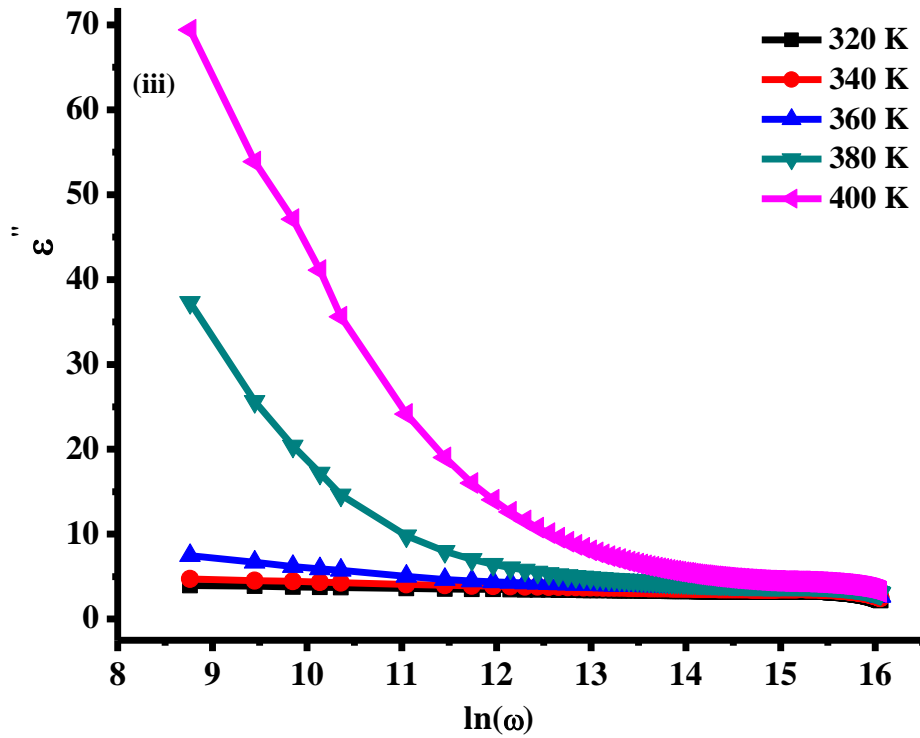
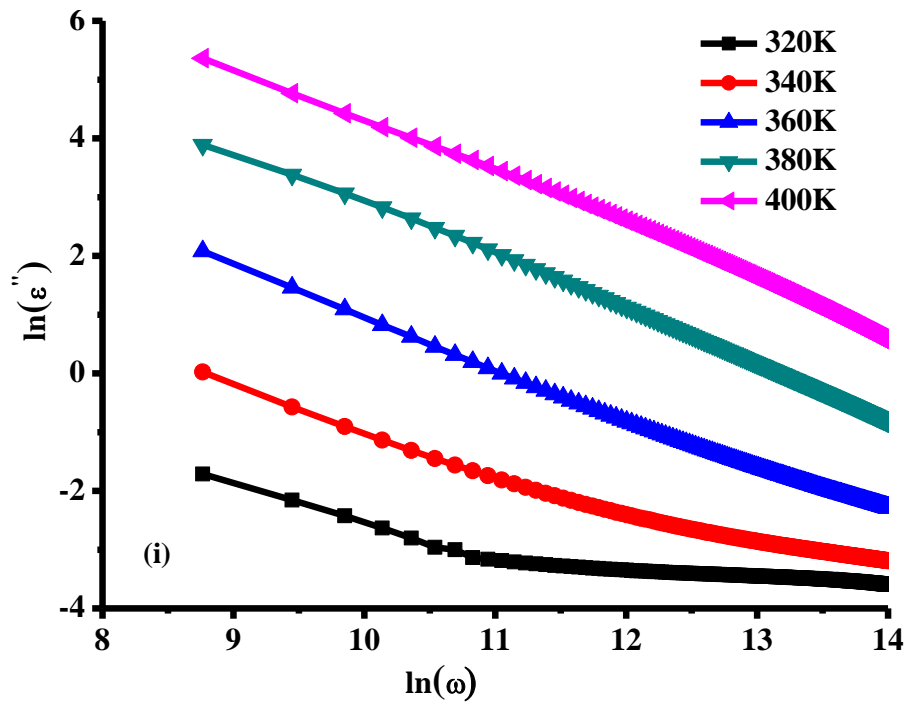
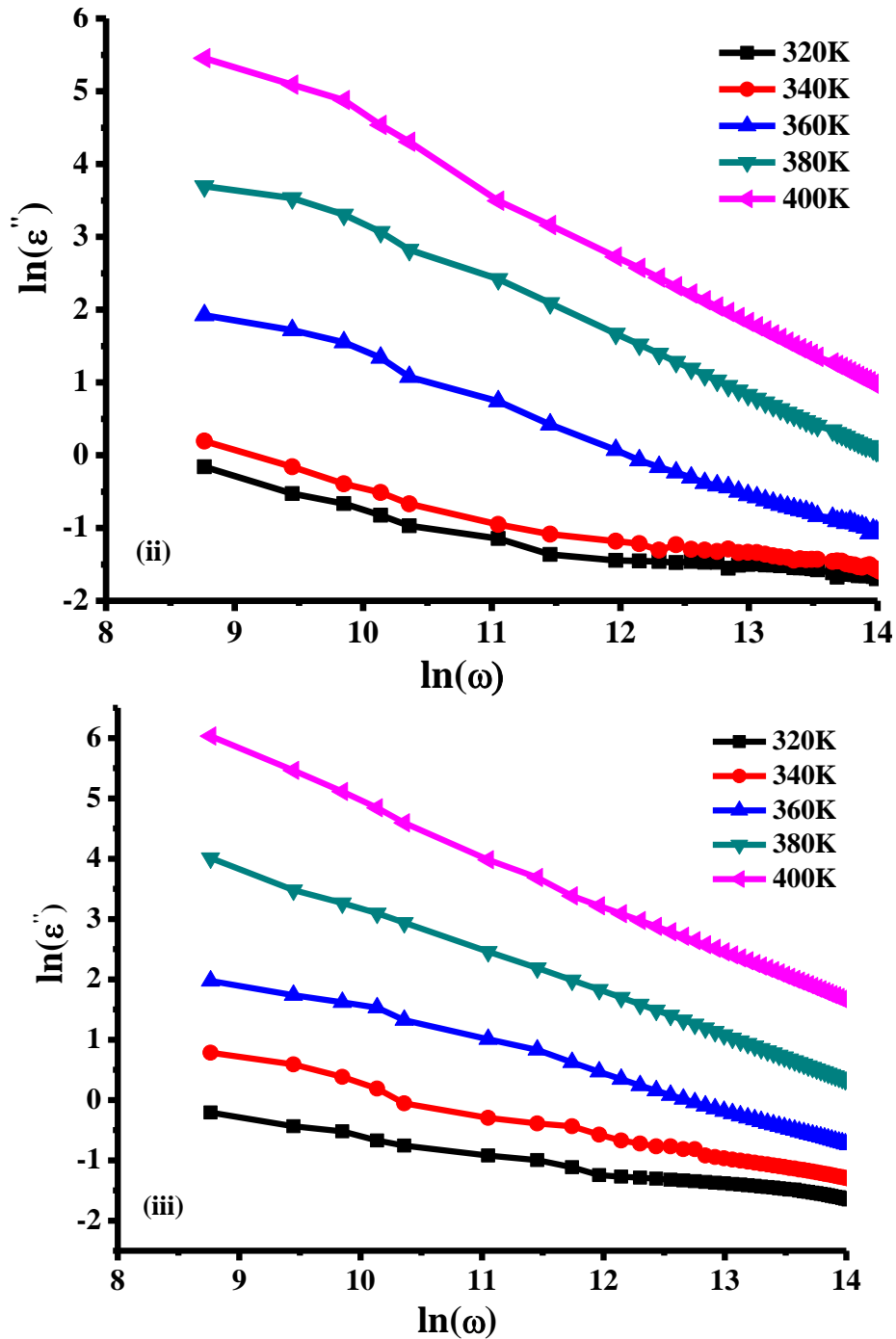
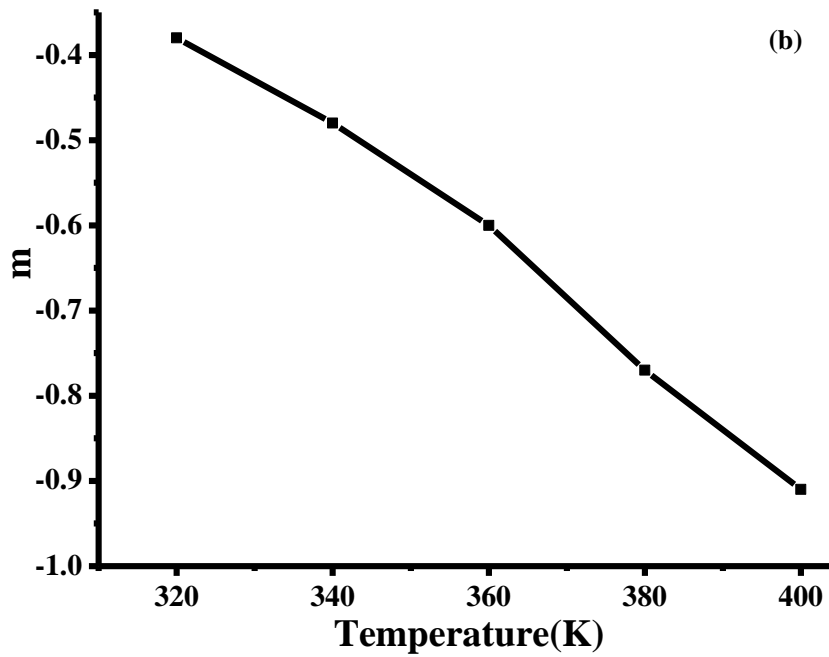
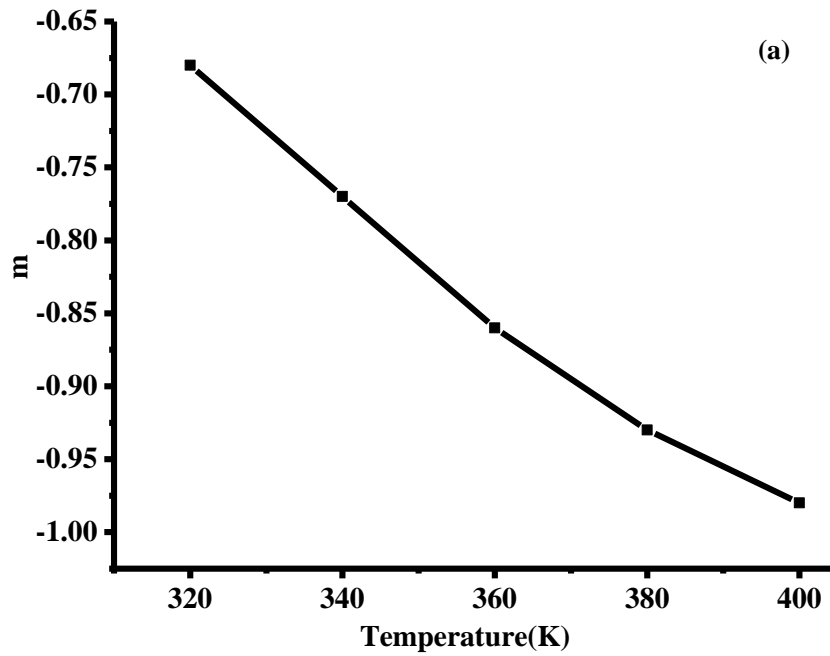


Figure 8 Variation of real part of dielectric permittivity with frequency for (i) PVA (ii) PVA+1% RGO (iii) PVA+2% RGO composites at different temperatures





**Figure 9** Variation of imaginary part of dielectric permittivity with frequency for (i) PVA (ii) PVA-1%RGO (iii) PVA-2%RGO composites at different temperatures



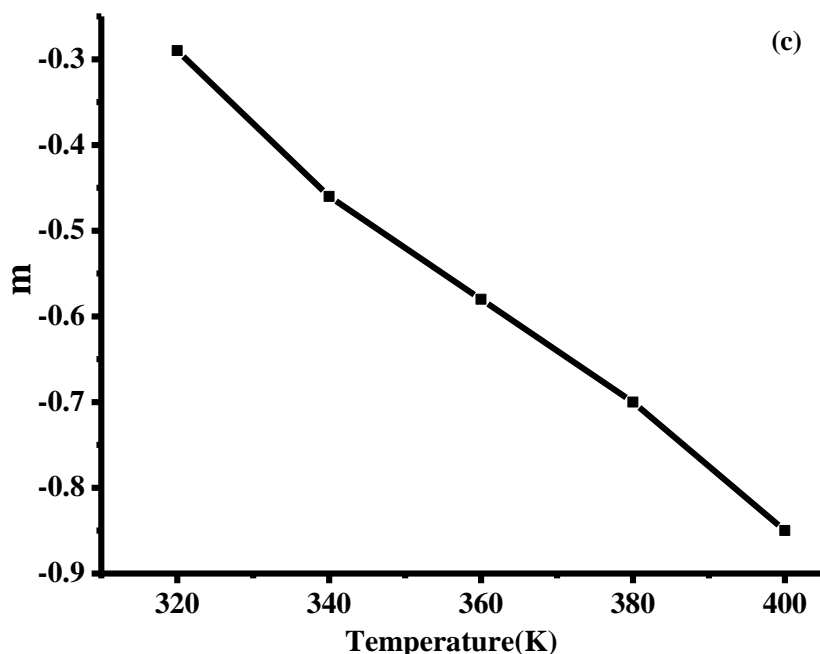


**Figure 10** Temperature dependence of power parameter m for (a) PVA (b) PVA+1% RGO (c) PVA+2% RGO composites

**Table1** Value of maximum barrier height for PVA and PVA-RGO composites

Sample	$W_m$ (eV)
PVA	0.38
PVA+1% RGO	0.29
PVA+2% RGO	0.16

<sup>i</sup> R. Zuo, X. Fang, C. Ye, Appl. Phys. Lett. 90, 092904(2007)

<sup>ii</sup> S. Sinha, S. Kumar Chatterjee, J. Ghosh, A.K. Meikap, Dielectric relaxation and ac conductivity behaviour of polyvinyl alcohol–HgSe quantum dot hybrid films J. Phys. D: Appl. Phys.47 (2014) 275301-2753012

<sup>iii</sup> C.U. Devi, A.K. Sharma, V.V.R.N. Rao, Electrical and optical properties of pure and silver nitrate-doped polyvinyl alcohol films Mater. Lett. 56 (2002) 167-174

<sup>iv</sup> N.B Halima, Poly(vinyl alcohol): Review of its promising applications and insights into biodegradation RSC Advances. 46(2016)1-33

<sup>v</sup> A.K. Geim and K.S Novoselov, The rise of graphene Nat Mater. 6 (2007) 183-191

<sup>vi</sup> K.I. Bolotin, K.J. Sikes, Z. Jiang, M. Klima, G. Fudenberg, J. Hone, P. Kim, H.L. Stormer, Ultra high mobility in suspended graphene Solid State Comm. 146 (2008) 351-355

<sup>vii</sup> Z. F. Li, H. Zhang, Q. Liu, L. Sun, L. A. Stanciu, J. Xie, Fabrication of high-surface-area graphene/polyaniline nanocomposites and their application in supercapacitors ACS Appl. Mater. Interfaces.9 (50) (2017)43939-43949

Viii Anthony J. Bur, Dielectric properties of polymers at micro wavefrequencies: a review, Polymers. 1985, 26(967-977)D Bur

<sup>ix</sup> Marco T. Connor,\* Saibal Roy,† Tiberio A. Ezquerra,‡ and Francisco J. Balta´ Calleja, Broadband ac conductivity of conductor-polymer composites, Physical review, 1998, 57(2286-2294)

<sup>x</sup> Subhojyoti Sinha • Sanat Kumar Chatterjee •Jiten Ghosh • Ajit Kumar Meikap, Electrical transport properties of polyvinyl alcohol–selenium nanocomposite films at and above room temperature, J Mater Sci

<sup>xi</sup> B.M. Greenhoe, M.K. Hassan, J.S. Wiggins, K.A. Mauritz, Universal Power Law Behavior of the AC Conductivity Versus Frequency of Agglomerate Morphologies in Conductive Carbon Nanotube-Reinforced Epoxy Networks JOURNAL OF POLYMER SCIENCE, PART B: POLYMER PHYSICS. 00 (2016) 000–000

<sup>xii</sup> W.S. Hummers, R.E. Offeman, Preparation of graphitic oxide J. Am.Chem. Soc. 80(6) (1958) 1339

- <sup>xiii</sup> J. I. Paredes, S. Villar-Rodil, A. Martinez-Alonso, J.M.D. Tascon, Graphene oxide dispersions in organic solvents *Langmuir*. 24 (2008) 10560–10564
- <sup>xiv</sup> L. Yang, Deslippe, C.H. Park, M.L. Cohen, S.G. Louie, Excitonic effects on the optical response of graphene and bilayer graphene *Phys. Rev. Lett.* 103, (2009) 186802
- <sup>xv</sup> T.F. Emiru, D.W. Ayele, Dispersion behaviour of graphene oxide and reduced graphene oxide. *Journal of colloid and interface science Controlled synthesis, characterization and reduction of graphene oxide: A convenient method for large scale production Egyptian Journal of Basic and Applied Sciences*. 4 (2017) 74–79
- <sup>xvi</sup> B. Gupta, N. Kumar, K. Panda, S. Dash, A.K. Tyagi, Energy efficient reduced graphene oxide additives: Mechanism of effective lubrication and antiwear properties *Scientific reports*. 6 (2016) 18372
- <sup>xvii</sup> C.S. Ramya, T. Savitha, S. Selvasekarapandian, G. Hirankumar, Transport mechanism of Cu-ion conducting PVA based solid-polymer electrolyte *Ionics*. 11(5) (2005) 436-441
- <sup>xviii</sup> W.K. Lee, J.F. Liu, A.S. Nowick, *Phys. Rev. Lett.* 67,1559 (1994).
- <sup>xix</sup> S.R. Elliott, *Adv. Phys.* 36, 135 (1987); *Solid State Ion.* 70-71, 27 (1994).
- <sup>xx</sup> K.C. Kao (2004), *Dielectric Phenomena in Solids with Emphasis on Physical Concepts of Electronic Processes*, Elsevier Academic Press,
- <sup>xxi</sup> N.A. Hegab, M.A. A., H.E. Atyia, M.I. Ismael, *Acta Phys. Pol. A* 119, 416 (2011).
- <sup>xxii</sup> H.M. El-Mallah, N.A. Hegab, *J. Mater. Sci.* 42, 336(2007).
- <sup>xxiii</sup> S.R. Elliott, *Adv. Phys.* 36, 135 (1987); *Solid State Ion.* 70-71, 27 (1994).
- <sup>xxiv</sup> Shang JW, Zhang YH, Yu L, Shen B, Lv FZ, Chu PK. Fabrication and dielectric properties of oriented polyvinylidene fluoride nanocomposites incorporated with graphene nanosheets. *Mater. Chem. Phys.* 2012;134:867–874.
- <sup>xxv</sup> K. S. Hemalatha, G. Sriprakash, M. V. N. Ambika Prasad, R. Damle, K. Rukmani, Temperature dependent dielectric and conductivity studies of polyvinyl alcohol-ZnO nanocomposite films by impedance spectroscopy *J. Appl. Phys.* 118 (2015) 154103
- <sup>xxvi</sup> T.V. Hung, G.S. Frank, Towards model-based engineering of optoelectronic packaging materials: dielectric constant modeling *Microelectronics Journal*. 33 (2002) 409-415
- <sup>xxvii</sup> F.H.A. El-kader, W.H. Osman, K.H. Mahmoud, M.A.F. Basha, Dielectric investigations and ac conductivity of polyvinyl alcohol films doped with europium and terbium chloride *Phys B*. 403 (2008) 3473–3484
- <sup>xxviii</sup> H.W. Gibsen, R.J. Weagley, W.M. Prest, Jr., R. Mosher, S. Kaplan, *J. Phys. Collo. C* 6 (suppl.),123 (1983).ω§